Soft Matter

PERSPECTIVE

Cite this: DOI: 10.1039/d6sm00234j

Role of hydration effects in driving ion binding to polyelectrolyte brushes and chains: a perspective

Raashiq Ishraaq and Siddhartha Das *

Polyelectrolyte (PE) chains and PE brushes are often characterized by the nature of the counterions that bind to them, as such binding regulates different properties of the chains and brushes. However, despite extensive research probing the properties of PE chains and brushes in the presence of a wide variety of counterions, the understanding of what would be the relative strength of binding of a specific type of counterion to a specific type of PE chain/brush remains elusive. In this perspective article, driven by our recent all-atom molecular dynamics (MD) simulations, we propose the following hypothesis that aims to fill this void: more chaotropic (kosmotropic) ions—those that disrupt (preserve) the surrounding water structure—tend to bind more strongly to polyelectrolyte (PE) chains and PE brushes bearing hydrophobic (hydrophilic) functional groups due to solvent mediated interactions. Therefore, our hypothesis accounts for the effect of hydration on ion binding to the PE brushes and chains: ions bind more favorably to PE chains/brushes having functional groups that impart a similar effect towards water. Subsequently, we discuss experimental and *ab initio* simulation results on counterion binding to PE chains and brushes from a large number of studies and establish the validity of our hypothesis by testing it against the findings of these studies. Finally, we identify the possible applications of our proposed hypothesis (in terms of designing systems that involve PE brushes and chains) and machine learning and density functional theory calculations that can further strengthen our understanding of the PE–counterion binding events.

Received 19th March 2026,
Accepted 10th May 2026

DOI: 10.1039/d6sm00234j

rsc.li/soft-matter-journal

A. Introduction

Charged polymers, namely polyelectrolytes (PEs), occurring in various forms such as chains, brushes, networks, complexes, gels, *etc.*, have kindled our imagination and excitement for many decades owing to their widespread applications in various facets of science, medicine, and engineering.[1–5] These PE chains and brushes are not present alone; rather, they are invariably present with a cloud of counterions that are screening their charges. Moreover, the charged nature of the PE chains, which are closely grafted (when these PE chains form brushes), imparts a highly charged confined environment to the surrounding solvent molecules and the counterions. Several of our previous studies have employed all-atom molecular dynamics simulations to establish that, due to such brush-imparted confinement, the properties of the PE brush-supported counterions and solvents (such properties include counterion mobility,[6–9] number of water–water hydrogen bonds,[6–15] water dipole moment,[6–15] water tetrahedral order parameter,[6–15] *etc.*) become severely distorted as compared to their properties in the bulk (*i.e.*, outside the PE brush layer). This greatly complicates the solvent–ion–PE brush interactions, leading to changes in the brush morphology in unexpected ways: for example, as shown in our previous study, the hydration of a brush functional group can get significantly affected depending on the nature of the counterions bound to the brush. Therefore, any model or description of the PE chains and brushes essentially needs to consider these counterions, the effects of solvents, and the intertwined relations between solvent–counterion–PE functional groups. In fact, the classical models of the PE chains often describe them in terms of the extent of influence of these counterions.[16–20] For example, PE chains or PE brushes are considered to be osmotic chains or osmotic brushes if the osmotic pressure of the counterions influences the overall configuration of these brushes and chains.[16] Similarly, the extent of the presence of the counterions determines the degree of deviation of several properties (*e.g.*, persistence length) of the PE chains as compared to the uncharged polymer chains.[21,22]

Research on PE brushes has been enriched by sustained contributions over the past several decades. These include a deep theoretical understanding of the topic developed through scaling laws (identifying the different regimes in which a PE brush can exist)[16,23–25] as well as more rigorous analytical and semi-analytical models providing a deep understanding of the monomer distribution, distribution of the chain ends, and the counterion

Department of Mechanical Engineering, University of Maryland, College Park, MD, 20742, USA. E-mail: sidd@umd.edu

distribution.[26–32] There is also a large volume of fundamental experimental,[33–37] coarse-grained[38–42] and atomistic[6–15] simulation studies that have provided an excellent understanding of the PE brushes. Interestingly, recent experimental and simulation studies have enriched our understanding of the PE brush–counterion–solvent or PE chain–counterion–solvent interactions to an extent that enables us to probe domains that are beyond the simplistic description of the PE–counterion interactions that are agnostic of the specific chemical nature of the counterions.[9,13,15,43–53] For example, classical ion-nature-agnostic theories cannot explain why two different types of monovalent counterions (or two different types of divalent counterions) bind with different strengths to a given type of PE brush (leading to different values of the equilibrium brush height). For example, Ji *et al.* showed that different halide ions bind to a particular cationic PE brush in a manner that is counter-intuitive if one considers the charge density of the halide counterions to be the main factor determining this strength of binding.[43] Similarly, PE brushes in the presence of counterions of different valences demonstrate behaviors that classical theories (agnostic of the nature of the counterions) fail to explain.[9,13,15,46–53]

In this perspective paper, we shed light on a missing aspect that is found to have a significant effect on determining counterion binding to the PE brushes and chains. This aspect is the hydration effect associated with both the counterions and the PE chains and brushes, or more specifically, the charged functional groups (of the chains and brushes) to which the counterions bind. The hydration effect related to the functional groups of the PE brushes and chains refers to the hydrophilic or hydrophobic nature of these groups. On the other hand, the hydration behavior of the counterions refers to their chaotropic or kosmotropic nature, *i.e.*, whether they disrupt their surrounding water structures (chaotropic ions) or they preserve their surrounding water structures (kosmotropic ions). Such nature of these ions determines their relative positions on the Hofmeister series: kosmotropes, positioned on the left of the Hofmeister series (see Fig. 1), interact strongly with water and are strongly hydrated, whereas chaotropes, positioned on the right of the series (see Fig. 1), are weakly hydrated.[54] These two classes of ions produce markedly different effects on protein stability and solubility, either indirectly through water-mediated interactions or directly through ion–protein binding.[55] Through several of our own papers on all-atom molecular dynamics (MD) simulations of PE brushes, we have shown that there is a strong dependence of the relative nature of the hydration properties of the brushes and the counterions on the strength of binding of the counterions to the brushes.[6–15,56–61] Our studies identify that even in a densely charged environment, the charged species (functional group and counterion) maintain their individual influence on the surrounding water structure, and the similarity in hydration strength is the dominant factor affecting binding between the counterion and the PE functional group.

In this article, we first discuss the vast number of studies probing the counterion binding to PE chains and brushes. Subsequently, we discuss our relevant all-atom MD simulation papers[11,13] and based on that introduce a generic hypothesis that connects such hydration behavior (of the brushes and chains and the counterions) to the strength of counterion binding to the brushes and chains (see Fig. 2). Next, and most importantly, we establish the validity of this proposed hypothesis by testing it against a vast number of existing experimental studies and *ab initio* calculations. Finally, we end by delving into some futuristic aspects of this problem, which include (1) the use of electronic calculations and machine learning to better understand the counterion–PE brush and counterion–PE chain binding events and (2) the potential applications of the proposed hypothesis in better explaining/designing several PE–ion binding events.

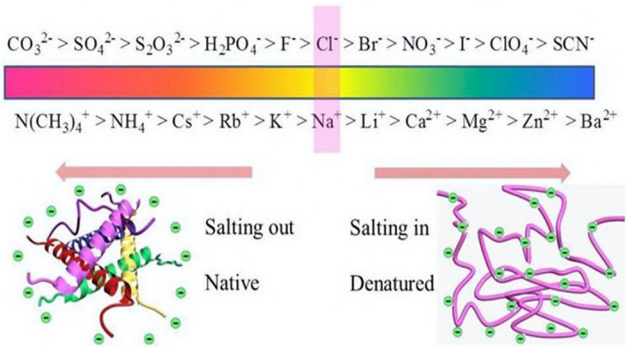

Fig. 1 Schematic of the Hoffmeister series: ions on the left (right) are kosmotropic (chaotropic) ions. This figure has been adapted from ref. 54 with permission from the American Chemical Society (B. Kang, H. Tang, Z. Zhao, and S. Song, Hofmeister series: insights of ion specificity from amphiphilic assembly and interface property, *ACS Omega*, 2020, **5**, 6229, copyright 2020).

Before going deeper into the paper, we would like to point out that the effect we discuss here (namely the hydration effect driven binding of counterions to the PEs) is an effect that is true for both the PE brushes and the PE chains. Later, we provide several examples, where we discuss studies that report how the PE chains show changes in their radii of gyration or hydration radii with changes in counterions. However, it must be pointed out that there are significantly more studies that have investigated the effect of counterion variation on the brush height than the dimensions (radius of gyration) of a PE chain. This is possibly due to the fact that the strong confinement effect imposed by the brushes[6,7] enables a more effective localization

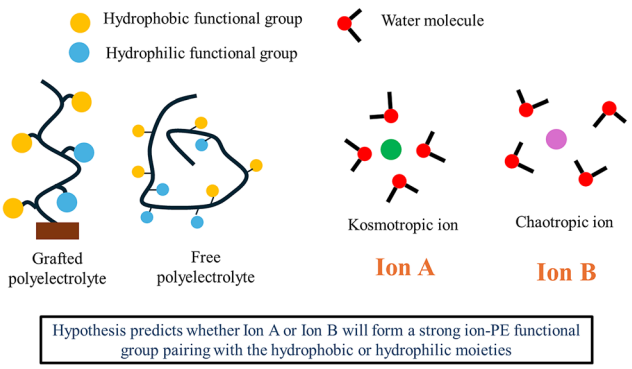

Fig. 2 Schematic illustration of how our hypothesis on the hydration effect dictates the ion binding inside PE brushes and PE chains. Fig. 5 and 6 provide the hypothesis in a schematic form in great detail.

(within the brush layer) of the counterions: this is evident from the very low mobility of the counterions inside the brush layer, as observed in several of our all-atom MD studies.[6,7] Therefore, there is a stronger manifestation of changes in brush height with changes in the type of binding counterions. In contrast, for the PE chains in a solvent, such confinement effects are absent and therefore, the localization of the counterions might not be so strong leading to a weaker manifestation of the change in the PE chain dimensions with the change in the nature of the counterions. Of course, there are papers focused on the collapse (or coil-to-globule transition) of a PE chain in a poor organic solvent in the presence of different counterions;[62–64] such a collapse, however, is more due to the presence of the poor solvent than the counterions. We have discussed such papers as well below.

B. Counterion–PE binding: examples from existing literature

PE chains and brushes are characterized by the counterions that bind to the PEs and screen the PE charges. In fact, there have been extensive studies focused on investigating the manner in which various PE chains and brushes change their configurations in the presence of different counterions. From these configurations, one can infer the relative strength of binding of the counterions to the PE brushes and chains. For example, for cases where the brush height is shorter (or the chain radius of gyration is smaller) in the presence of a given type of counterion, it is inferred that the binding of the corresponding counterions to the PE brushes (or the PE chains) must be stronger. Such stronger binding leads to more effective screening of PE brush (PE chain) charges, resulting in weaker inter-monomeric repulsion and a reduced PE brush height (or a reduced PE chain radius of gyration). Some of these results on the binding of different counterions to different types of PE brushes and chains have been discussed below. Typically, such counterions are not added separately: the researchers consider the presence of a salt and the ion of the salt (cation or anion) that has the charge opposite to the PE charges as the "counterions" and these counterions go and bind to the oppositely charged functional groups of the PE brushes. For example, for cationic $PMETA^+$ (poly[2-(methacryloyloxy)-ethyltrimethyl ammonium]) brushes, when NaCl salt solution is added, the Cl^- ion is the counterion (as its charge is opposite to that of $PMETA^+$) and the Na^+ ion is the coion. More specifically, the added salt enters the brush layer and the ions (cation or anion part of the salt) get ionized from the salt and bind to the PE brush functional groups. To be even more rigorous, given the fact that the system overall must always be charge neutral, the brush layer, in the absence of the salt, might have ions from water (H_3O^+ or OH^-) that very weakly screen the PE brush charges; these water ions are replaced by the salt ions when they are added. In several of our all-atom MD papers,[57,58] we have studied the distribution of such screening counterions and salt ions entering the brush layer and those remaining outside the brush layer. Often, factors like the overall osmotic pressure of the system, the grafting density of the brushes, steric hindrance imparted by the bulky side groups of the brushes, the degree of ionization of the brushes, *etc.* dictate the overall changes in entropy (which typically decreases) and changes in enthalpy (which typically decreases for favorable binding) associated with the migration of salt from the bulk to the brush layer and the subsequent binding of the counterions to the brushes. This relative interplay of the changes in the entropy and enthalpy eventually decides what fraction of the added salt is inside or outside the brush layer.

B.1. Binding of anions to cationic brushes

Ji *et al.* inferred that the strength of binding between cationic $PMETA^+$ (poly[2-(methacryloyloxy)-ethyltrimethyl ammonium]) brushes and halide ions varies as: $I^- > Br^- > Cl^- > F^-$ (obviously, these halide ions behave as the corresponding counterions).[43] They arrived at this conclusion by noting that the $PMETA^+$ brush height (h_b) decreased with the halide ion in the order as $(h_b)_{I^-} < (h_b)_{Br^-} < (h_b)_{Cl^-} < (h_b)_{F^-}$.[43] In this study, three separate grafting densities were considered: 0.02, 0.03, and 0.05 chains per nm^2. Also, the substrates considered here were silicon wafers and gold-coated solid substrates, while the molecular weight of the brushes was 205×10^3 g mol^{-1}. Also, the solvent used was the aqueous solution of the salt Na–X (X = I^-, Br^-, Cl^-, and F^-) with concentrations varying from 10^{-4} M to 5 M. Thus, these anions coming from the Na–X salt served as the corresponding counterions, as discussed above. Finally, it must be noted that this behavior $(h_b)_{I^-} < (h_b)_{Br^-} < (h_b)_{Cl^-} < (h_b)_{F^-}$ was reported for the entire salt concentration range (10^{-4} M to 5 M), but only for the grafting density of 0.05 chains per nm^2. Variation of the brush height for smaller grafting densities was not reported.

Kou *et al.* showed that $PMETA^+$ brush height is smaller in the presence of SCN^- ions (thiocyanate ions), as compared to that in the presence of SO_4^{2-} ions (*i.e.*, when the counterion is changed from the SCN^- ion to the SO_4^{2-} ion). As a consequence, they inferred that the SCN^- ion binds more strongly than the SO_4^{2-} ion to the $PMETA^+$ brushes.[44] The substrate considered was a silica-coated resonator surface, while the solvent was an aqueous solution of NaSCN and Na_2SO_4 at different salt concentrations (0.001, 0.01, 0.1, and 0.5 M), and this height difference between SCN^--counterion screened $PMETA^+$ brushes and SO_4^{2-}-counterion screened $PMETA^+$ brushes was observed for all salt concentrations.

Ehtiati *et al.* conducted experiments to probe the interactions of the cationic poly[2-(1-butylimidazolium-3-yl)ethyl methacrylate] brushes with various counterions (for two different brush grafting density values, namely 0.25 nm^{-2} and 0.08 nm^{-2}), including SCN^- ion, and hypothesized that the SCN^- ion bound most strongly to these brushes leading to the least swelling (attainment of least height) by these brushes in the presence of SCN^- ion.[45] In fact, they inferred that the strength of the binding of the anions to the cationic poly[2-(1-butylimidazolium-3-yl)ethyl methacrylate] brushes varied as: $SCN^- > NO_3^- > Br^- > Cl^-$ (especially for a grafting density of 0.25 nm^{-2}). Their inference was based on the fact that the height of the poly[2-(1-butylimidazolium-3-yl)ethyl methacrylate] brush (as a function of the nature

of the counterions) varied as: $(h_b)_{SCN^-} < (h_b)_{NO_3^-} < (h_b)_{Br^-} < (h_b)_{Cl^-}$.[25] Obviously, the corresponding solution for these cases was Na–X (X = SCN^-, NO_3^-, Br^-, and Cl^-) salt solution of concentrations varying from 10^{-4} M to 1 M. There is, however, an anomaly for the case of smaller grafting densities and smaller concentrations. For that case (grafting density of 0.08 nm^{-2} and salt concentrations of less than 0.1 M), the brush height varied as: $(h_b)_{SCN^-} < (h_b)_{Br^-} < (h_b)_{NO_3^-} < (h_b)_{Cl^-}$, implying that the corresponding strength of binding varied as: $SCN^- > Br^- > NO_3^- > Cl^-$.[15] Of course, for the same grafting density at salt concentrations of 0.1 M or higher, the same trend, namely, $(h_b)_{SCN^-} < (h_b)_{NO_3^-} < (h_b)_{Br^-} < (h_b)_{Cl^-}$, as that obtained for larger grafting density, was recovered. For all the cases, the substrate on which the brushes were grafted was a silicon wafer.

He *et al.* studied the ion binding on the poly-zwitterionic (PZI) poly(cysteine methacrylate) (PCysMA) brushes[65] at a brush grafting density of 0.1 chains per nm^2. The brushes (molecular weight of 584 kg mol^{-1}) contained a cationic NH_3^+ group and an anionic COO^- group. Here we first discuss the binding of the anions to the NH_3^+ group of PZI. It was inferred that the strength of binding of the anions (to the cationic NH_3^+ group of PZI) varied as: $SO_4^{2-} > Cl^- > NO_3^- \sim Br^- > SCN^-$, stemming from the fact that the brush height varied as: $(h_b)_{SO_4^{2-}} < (h_b)_{Cl^-} < (h_b)_{NO_3^-} \sim (h_b)_{Br^-} < (h_b)_{SCN^-}$.[65] The solution was the aqueous salt solution of the salt Na–X (X = Cl^-, NO_3^-, Br^-, and SCN^-) and Na_2SO_4 having concentrations ranging from 10^{-6} M to 3 M. This distinct variation in the brush height with the variation in the counterion was observed primarily for salt concentrations ranging from 0.1 to 3 M; for smaller salt concentrations, the differences in the brush height (and therefore, the binding strength) were not significant.

B.2. Binding of cations to anionic brushes

Ji *et al.* studied the binding of the alkali cations to the anionic PSS (poly-styrene sulfonate) brushes and reported that the binding strength varied as: $Cs^+ > K^+ > Na^+ > Li^+$ (obviously, these alkali ions behave as the corresponding counterions), stemming from the fact that the brush height (in the presence of counterions) varied as $(h_b)_{Cs^+} < (h_b)_{K^+} < (h_b)_{Na^+} < (h_b)_{Li^+}$.[43] For this study, three separate grafting densities of the PSS brushes were considered: 0.01, 0.02, and 0.04 chains per nm^2. Also, the substrates considered here were silicon wafers and gold-coated solid substrates, while the molecular weight of the brushes was 218×10^3 g mol^{-1}. Also, the solvent used was the aqueous solution of the salt Y–Cl (Y = Cs^+, K^+, Na^+, and Li^+) with concentrations varying from 10^{-4} M to 5 M. Finally, it must be noted that this behavior $(h_b)_{Cs^+} < (h_b)_{K^+} < (h_b)_{Na^+} < (h_b)_{Li^-}$ was reported for the entire salt concentration range (10^{-4} M to 5 M), but only for the grafting density of 0.04 chains per nm^2. Variation of the brush height for smaller grafting densities was not reported.

In the study of the ion binding to the PZI brush [poly-(cysteine methacrylate) (PCysMA)], He *et al.* reported a smaller brush height with Ca^{2+} salt compared to Ba^{2+} salt.[65] This indicated that the Ca^{2+} (Ba^{2+}) ion bound more strongly (weakly) to the COO^- group (anionic group) of the PZI brush. The solution was the aqueous salt solution of the salt Y–$(NO_3)_2$ (Y = Ca^{2+} and Ba^{2+}) with concentrations ranging from 10^{-6} M to 1 M. This distinct variation in the brush height with the variation in the counterion was observed for nearly the entire range of the salt concentration. Other quantities (*e.g.*, grafting density, molecular weight of the brushes, nature of the substrate, *etc.*) have been already discussed above.

Xu *et al.* reported that the strength of binding of the divalent cations to the PSS brushes varied as: $Ba^{2+} > Ca^{2+} > Mg^{2+}$, stemming from the fact that the PSS brush height (as a function of the counterions) varied as: $(h_b)_{Ba^{2+}} < (h_b)_{Ca^{2+}} < (h_b)_{Mg^{2+}}$.[66] The results considered a mica surface (with a brush grafting density of 0.025 chains per nm^2) and a silicon surface (with a brush grafting density of 0.1 chains per nm^2). Also, the solution was the aqueous salt solution of Y–$(NO_3)_2$ (Y = Mg^{2+}, Ca^{2+}, and Ba^{2+}) with the salt concentration varying from 0.003 to 0.3 M. This height variation was noted for the entire range of the salt concentrations (0.003 to 0.3 M) for the case of the silicon substrate (with a brush grafting density of 0.1 chains per nm^2). The molecular weight of brushes was 70 000 g mol^{-1}.

In addition to standard PE brushes, there are several other examples where the effect of ion binding on other negatively charged macromolecules forming brush-like configurations has been probed. Bracha *et al.*, for example, considered a 968-base-pair DNA brush grafted on a rectangular pattern in a manner such that its grafting density progressively increased along the grafting surface.[67] It was found that as the counterions was changed from Na^+ to Mg^{2+}, the brush height decreased for all values of grafting densities and all salt concentrations (the solvent was a solution of the chloride salts of these counterions, and the salt concentration varied from 0.2 to 150 mM). Other studies include probing the changes in the height of spherical DNA brushes (DNA brushes grafted to silver nanoparticles) in the presence of two different ionic liquids (namely, [BMIM] acetate and [EMIM] acetate): the DNA brush height reduced for all values of ionic liquid concentrations when the liquid was changed from EMIM acetate to BMIM acetate.[68]

There are also examples of considering ion binding to protein brushes. For example, Srinivasan *et al.* probed the height of an IDP (intrinsically disordered protein), based on a neurofilament complex, present in the form of brushes in the presence of varying concentrations of sodium-chloride salt.[69] Yokokura *et al.* developed a theory to explain such salt concentration response of protein brushes.[70]

Finally, Pradal *et al.* probed the height variation of the polysaccharide (in the form of different types of pectin) brushes in the presence of different concentrations of the sodium chloride salts.[71] Most of these studies (with the exception of the paper by Bracha *et al.*[67]) did not explicitly provide the effect of varying the nature of the salt (or more specifically, the nature of the counterions) in changing the brush height. Therefore, these studies, while serve as very good examples of different types of PE brushes (or brushes of the charged biological macromolecules) showing distinct behaviors due to ion binding, will be of less use in establishing our hypothesis (discussed below).

B.3. Binding of cations to anionic PE chains

Li^+ ions have been found to bind more strongly than Cs^+ ions to PAA (poly-acrylic acid) chains, as evidenced by the stronger collapse (which is equivalent to a very small radius of gyration) of the PAA chains in the presence of Li^+ ions as compared to that in the presence of Cs^+ ions.[72] These findings were made from molecular dynamics (MD) simulations, which considered water–ethanol solution as the solvent and varied the volume fraction of ethanol from 0.1 to 0.9. Cs^+-ion-screened PAA chains were found to have a greater radius of gyration than the Li^+-ion-screened PAA chains for solutions corresponding to all volume fraction values of the ethanol.

Similarly, *ab initio* MD calculations showed that K^+ ions bind more strongly than the Na^+ ions to the PSS chains (using the corresponding RDF or the radial density function data).[73]

In addition to simple chains, there are examples of gels based on PAA chains: these gels (containing different types of organic solvents) have shown a larger swelling in the presence of 0.1 M solution of CsCl salt as compared to that in the presence of 0.1 M solution of NaCl salt for pH values of 5 and 12; however, this trend reverses for pH = 3.[74] Also, there are papers that study the collapse (or coil-to-globule transition) of the PE chains as a function of the concentration of different organic solvents in the presence of different counterions (or salts that furnish those counterions) for PE chains such as poly(styrene-*alt*-maleic acid) (PSaltMA), poly(acrylic acid) (PAA), poly(styrene sulfonate)s (PSS) and poly(vinyl sulfonate)s (PVS).[62–64] These papers[62–64,74] provide a very insightful understanding of the behavior of the PE chains in the presence of different ions: however, given the significant role of the organic solvents in most of these studies, they are of lesser value in establishing our hypothesis focusing just on the role of hydration of the counterions and the PE functional groups.

B.4. Binding of anions to cationic PE chains

In the PZI PE chain, PAEDAPS [(poly(3-[2-(acrylamido)ethyldimethylammonio]propanesulfonate))], the trimethyl ammonium group, is the cationic part. It was inferred that the strength of binding counterions to the PAEDAPS PZI chain (or more specifically, the strength of binding to the cationic part of the PZI) varied as: $SCN^- > ClO_4^- > NO_3^- > Br^- > Cl^- > SO_4^{2-}$, as evidenced by the fact that the hydration radius or R_h of the PZI (with these different counterions) varied as: $(R_h)_{SCN^-} < (R_h)_{ClO_4^-} < (R_h)_{NO_3^-} < (R_h)_{Br^-} < (R_h)_{Cl^-} < (R_h)_{SO_4^{2-}}$.[75] In this study, aqueous solutions of sodium salts of these anions were used as the solvent, with salt concentrations varying from 0.1 to 2 M. Distinct variation in the chain hydration radius (with the variation in the counterions) was noted when the results corresponding to solutions with salt concentrations from 0.8 to 2 M are averaged. For smaller salt concentrations, such variation was not very prominent.

Also, *ab initio* MD calculations have shown that Br^- ions bind more strongly than the Cl^- ions to the PDADMA [poly(diallyldimethylammonium)] chains.[73]

Finally, like the case of anionic PE chains collapsing in the presence of poor solvents and counterions, there are also papers investigating the collapse of the cationic PE chains in the presence of a poor solvent and counterions.[76] These studies are important in the literature of the counterion–PE chain interactions; however, they are of lesser value in establishing our hypothesis focusing on the role of hydration effects in the interaction between the PE chains and counterions.

C. The role of hydration effects in counterion binding to polyelectrolyte brushes revealed by all-atom molecular dynamics simulations

In the papers discussed in the previous section, there was little consideration of the hydration effect associated with the PE brushes or chains (or more specifically, the charged functional groups of the PE brushes or PE chains) and the hydration effect associated with the counterions. As a result, many of the findings of these papers, which appeared highly non-intuitive, could not be explained. For example, Ji *et al.* confirmed that the extent of binding of the halide ions to the $PMETA^+$ brushes varied as: $I^- > Br^- > Cl^- > F^-$;[43] this is counter-intuitive since the fluoride ion (iodide ion) being the smallest (largest) has the highest (smallest) charge density, and therefore one would expect the binding strength to vary as $I^- < Br^- < Cl^- < F^-$.

We carried out all-atom MD simulations to resolve this specific scenario (see Fig. 3).[13] It was confirmed (*via* radial density functional plots) that indeed the binding strength of the halide ions to the $PMETA^+$ brushes varied as $I^- > Br^- > Cl^- > F^-$ and consequently, the $PMETA^+$ brush height (h_b) varied as follows with the different halide counterions: $(h_b)_{I^-} < (h_b)_{Br^-} < (h_b)_{Cl^-} < (h_b)_{F^-}$ [see Fig. 3(e and f)]. This finding validated the experimental finding of Ji *et al.*[43]

In a previous paper,[11] we studied the hydration behavior of the $\{N(CH_3)_3\}^+$ group of the $PMETA^+$ brushes: it was demonstrated that inside the brush layer, due to the hydrophobic nature of the three methyl groups, the $\{N(CH_3)_3\}^+$ group formed and maintained an apolar (hydrophobic) hydration layer despite the positive charge of the $\{N(CH_3)_3\}^+$ group. As a consequence, the Cl^- ions (serving as the screening counterion), which are known to have a tightly bound hydration shell [confirmed by the corresponding Cl–O_w RDF; see Fig. 4(a)], could only weakly bind to the $\{N(CH_3)_3\}^+$ group. Accordingly, one can note that the N–Cl radial distance is more than the N–O_w radial distance with "N" representing the nitrogen atom of the $\{N(CH_3)_3\}^+$ group and "O_w" representing the oxygen atom of the water molecule [see Fig. 4(b)].

In our paper,[13] we provided an explanation of the specific binding tendencies of the different halide ions to the $\{N(CH_3)_3\}^+$ group of the $PMETA^+$ brushes by invoking this knowledge of the hydrophobic nature of the $\{N(CH_3)_3\}^+$ group of the $PMETA^+$ brushes (as revealed in ref. 11). Among the halide ions, iodide and bromide ions are chaotropic ions that disrupt the water

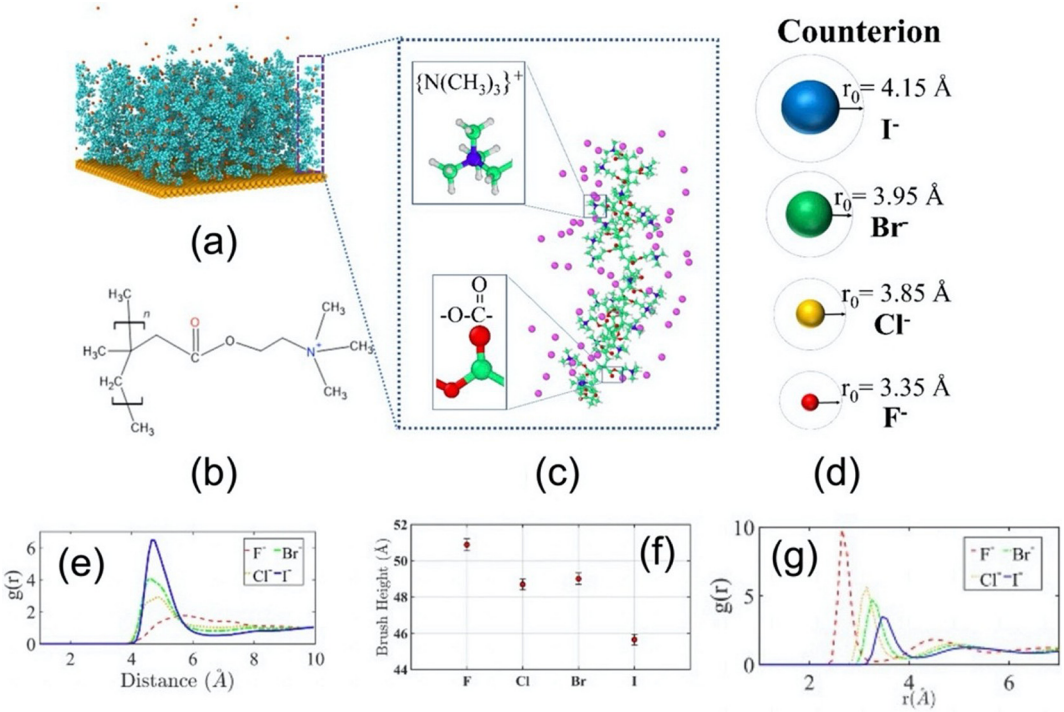

Fig. 3 (a) A schematic of the PMETA$^+$ brush system. Cyan, red, and orange spheres, respectively, denote the brush monomers, counterions, and wall atoms. (b) Chemical structure of the monomer. (c) A detailed structure of the polymer chain and the functional groups. Green, white, red, blue, and purple spheres, respectively, denote the carbon, hydrogen, oxygen, nitrogen, and halide counterions. (d) Representation of the sizes of the different halide counterions and their solvation shells. (e) RDFs of $\{N(CH_3)_3\}^+$–X (X = I^-, Br^-, Cl^-, and F^-). (f) PMETAX brush height variation in the presence of different halide ions. (g) X–O_w RDF inside the PMETAX brush layer (X: F^-, Cl^-, Br^-, and I^-; O_w: oxygen atom of the water molecule). Results shown in (e)–(g) are from the different all-atom MD simulations of the PMETA$^+$ brushes screened with X^- ions (X = I^-, Br^-, Cl^-, and F^-). All the subfigures of this figure have been reproduced from ref. 13 with permission from the American Chemical Society (R. Ishraaq and S. Das, All-atom molecular dynamics simulations of cationic polyelectrolyte brushes in the presence of halide counterions, *Macromolecules*, 2024, **57**, 3037, copyright 2024).

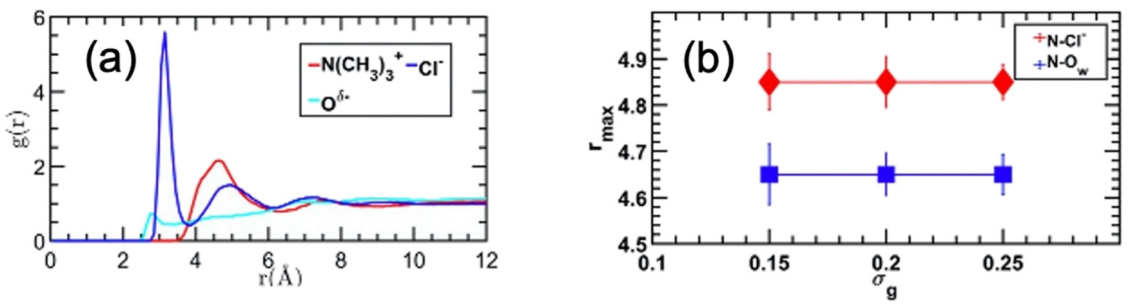

Fig. 4 (a) N–O_w, Cl^-–O_w, and $O^{\delta-}$–O_w RDFs. (b) Values of the locations of the peaks (r_{max}) of the N–O_w and N–Cl^- RDFs plotted as functions of the PMETA$^+$ grafting densities. These results are from the all-atom MD simulations of the PMETA$^+$ brushes screened with Cl^- ions. In (a) and (b), "*N*" represents the nitrogen atom of the $\{N(CH_3)_3\}^+$ group of the PMETA$^+$ brushes, $O^{\delta-}$ represents the oxygen atom of the carboxylate group of the PMETA$^+$ brushes, and O_w is the water oxygen atom. All the subfigures of this figure have been reproduced from ref. 11 with permission from the American Chemical Society (R. Ishraaq, T. S. Akash, A. Bera, and S. Das, Hydrophilic and apolar hydration in densely grafted cationic brushes and counterions with large mobilities, *J. Phys. Chem. B*, 2024, **128**, 381, copyright 2023).

structure around them; in other words, they do not form strong hydration layers, as confirmed by the corresponding I–O_w and Br–O_w RDFs [see Fig. 3(g)]. On the other hand, fluoride and chloride ions are kosmotropic ions, and therefore they do not disrupt the water structure and form strong hydration layers around them [also confirmed by the F–O_w and Cl–O_w RDFs; see Fig. 3(g)]. Under such circumstances, by invoking Collin's law of matched water affinity,[77] we could explain that oppositely charged entities that show similar (dissimilar) behavior towards water will bind strongly (weakly) to one another. This enabled us to explain why the strength of binding of the halide ions to the PMETA$^+$ brushes (containing hydrophobic functional groups) varied as $I^- > Br^- > Cl^- > F^-$ (*i.e.*, in the descending order of the chaotropic nature of the ions).

D. Our hypothesis on the role of the hydration effect in counterion binding to polyelectrolytes tested against existing studies

Based on our MD simulation findings (please see the previous section), we make the following hypothesis that govern the ion binding to the PE brushes and chains: more chaotropic (kosmotropic) ions bind more strongly (weakly) to the PE chains and brushes with hydrophobic functional groups. Conversely, the more chaotropic (kosmotropic) ions bind more weakly (strongly) to the PE chains and brushes with hydrophilic functional groups. As a consequence, the height of the PE brushes or the radius of gyration or hydration radius of the PE chains for the brushes and chains with hydrophobic (hydrophilic) functional groups are smaller (larger) in the presence of more chaotropic (kosmotropic) ions. Fig. 5 and 6 provide a pictorial summary of this hypothesis for the cases of the PE brushes and the PE chains, respectively.

In Table 1, we show how one can use this hypothesis to explain the various findings of ion binding to the PE brushes and PE chains (discussed in section B).

E. Future studies: electronic calculations, machine learning, and applications

E.1. Electronic calculations

Our all-atom MD simulation paper had explained the role of the solvent molecules around different chaotropic and kosmotropic

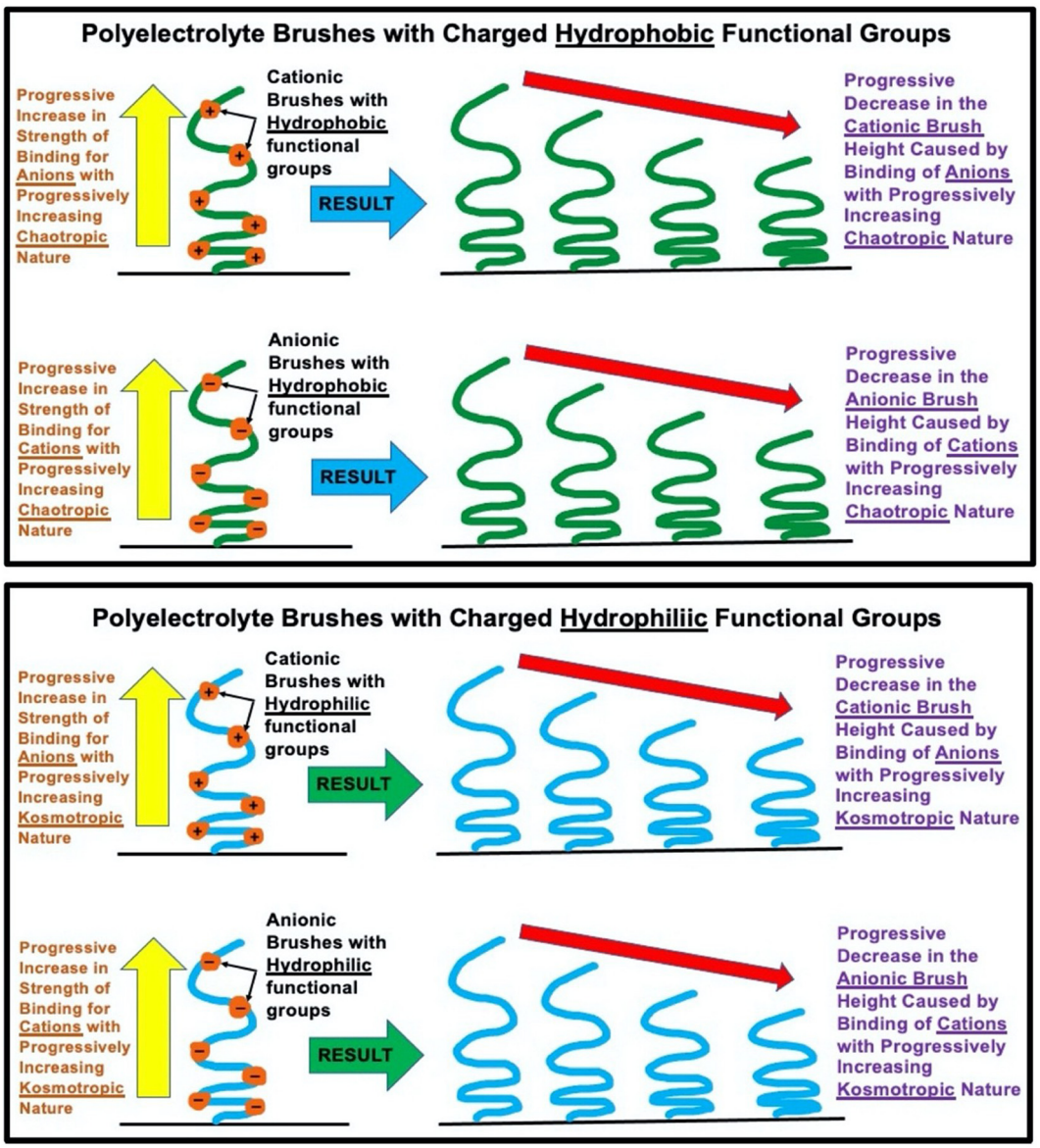

Fig. 5 Schematic representation of our hypothesis relating the ion binding to the PE brushes with hydrophobic functional groups (top panel) and hydrophilic functional groups (bottom panel). According to our hypothesis, for the PE brushes with hydrophobic (hydrophilic) functional groups, there is a progressive increase in the strength of binding (to the functional groups) of the more chaotropic (kosmotropic) ions, resulting in a progressive decrease in the height of the PE brushes.

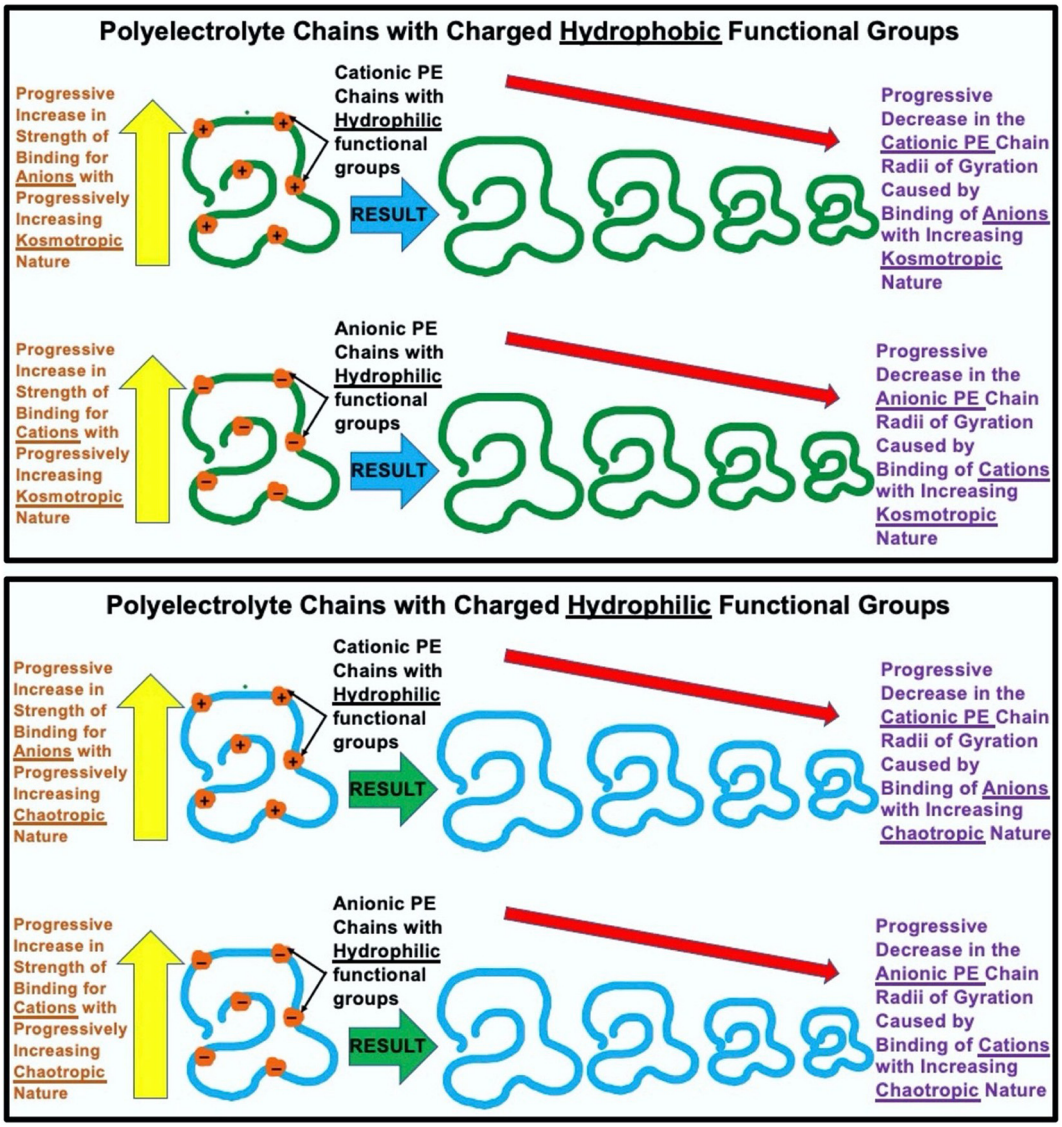

Fig. 6 Schematic representation of our hypothesis relating the ion binding to the PE chains with hydrophobic functional groups (top panel) and hydrophilic functional groups (bottom panel). According to our hypothesis, for the PE chains with hydrophobic (hydrophilic) functional groups, there is a progressive increase in the strength of binding (to the functional groups) of the more chaotropic (kosmotropic) ions, resulting in a progressive decrease in the radius of gyration of the PE chains.

halide counterions (*i.e.*, accounted for the solvent structure around the ions) in determining the strength of binding of these ions to the $PMETA^+$ brushes containing the hydrophobic $\{N(CH_3)_3\}^+$ functional group.[13] While the all-atom MD simulations can shed light on the effect of the solvent on the binding of different types of ions on PE brushes (or PE chains), there are several additional factors (beyond the scope of all-atom MD simulations) that can further elucidate specific ion-chemistry-dependent binding of counterions to the PE brushes and chains. In a recent paper,[79] we employed density functional theory (DFT) calculations (to obtain the electron density) (see Fig. 7) followed by QTAIM (quantum theory for atoms in molecules) analysis[80,81] to reveal the binding mechanism of the SCN^- ion (a highly chaotropic ion; even more chaotropic than the I^- ion) to the $PMETA^+$ brushes (see Fig. 7). It was revealed, most intriguingly, that the SCN^- ion interacts with three binding sites of the $\{N(CH_3)_3\}^+$ group of the $PMETA^+$ monomer; more specifically, the S-atom (of the SCN^- ion) interacts *via* two sites, while the N-atom (of the SCN^- ion) interacts *via* one site [see Fig. 7(c)]. As a result, the SCN^- counterion undergoes multidentate binding (similar to chelate formation) to the $\{N(CH_3)_3\}^+$ group of the $PMETA^+$ monomer. Also, this DFT-QTAIM framework was used to probe the non-covalent interactions (NCI) associated with the binding of the SCN^- ion with the $\{N(CH_3)_3\}^+$ group. For that purpose, we plotted the RDG (reduced density gradient) as a function of the quantity "$[\mathrm{sign}(\lambda_2)]\cdot\rho(\boldsymbol{r})$". Here $\rho(\boldsymbol{r})$ is the electron density distribution (obtained from the DFT calculations) and λ_2 is the second eigenvalue of the hessian matrix of ρ. Thus, the sign of λ_2 distinguishes bonded/attractive regions ($\lambda_2 < 0$) from the non-bonded/repulsive ones ($\lambda_2 > 0$). In the RDG($\boldsymbol{r}$) *vs.* "$[\mathrm{sign}(\lambda_2)]\cdot$

Table 1 Use of the proposed hypothesis (see above) for explaining the results from different studies on ion binding to PE chains and PE brushes

Ref.	Result	Explanation of the result using our hypothesis
Ji *et al.* (ref. 43)	The strength of binding between the cationic $PMETA^+$ brushes and halide ions varies as: $I^- > Br^- > Cl^- > F^-$	The functional group [$\{N(CH_3)_3\}^+$ group] of the $PMETA^+$ brushes is hydrophobic; therefore, the ions that are more chaotropic (kosmotropic) bind more strongly (weakly) to the $PMETA^+$ brushes (the degree of chaotropy decreases from I^- ion to F^- ion).
Kou *et al.* (ref. 44)	The SCN^- ion binds more strongly than the SO_4^{2-} ion to the $PMETA^+$ brushes	The functional group [$\{N(CH_3)_3\}^+$ group] of the $PMETA^+$ brushes is hydrophobic; therefore, the ions that are highly chaotropic (SCN^- ions) will bind more strongly than the ions that are highly kosmotropic (SO_4^{2-} ions) to the $PMETA^+$ brushes.
Ehtiati *et al.* (ref. 45)	The strength of binding of the anions to the cationic poly[2-(1-butylimidazolium-3-yl)ethyl methacrylate] brushes varies as: $SCN^- > NO_3^- > Br^- > Cl^-$	The positively charged N atom [of the poly[2-(1-butylimidazolium-3-yl)ethyl methacrylate] brushes], very much like the N^+ in the $PMETA^+$ brushes, is surrounded by saturated (or unsaturated) alkyl groups. As a result, the functional group for the cationic poly[2-(1-butylimidazolium-3-yl)ethyl methacrylate] brushes is also expected to be phobic. The degree of chaotropic nature of the ions varies as: $SCN^- > NO_3^- > Br^- > Cl^-$. Thus, the strength of binding of the ions to poly[2-(1-butylimidazolium-3-yl)ethyl methacrylate] varies as: $SCN^- > NO_3^- > Br^- > Cl^-$.
He *et al.* (ref. 65)	The binding strength of anions on the poly-zwitterionic poly(cysteine methacrylate) (PCysMA) brushes varies as: $SO_4^{2-} > Cl^- > NO_3^- \sim Br^- > SCN^-$	PCysMA brushes contain a cationic NH_3^+ group and an anionic COO^- group. The NH_3^+ group is a hydrophilic group, while the degree of kosmotropic nature of ions varied as $SO_4^{2-} > Cl^- > NO_3^- \sim Br^- > SCN^-$, explaining why the binding strength of the anions to the PCysMA brushes varies as: $SO_4^{2-} > Cl^- > NO_3^- \sim Br^- > SCN^-$.
Ji *et al.* (ref. 43)	The binding strength of alkali cations to anionic PSS (poly-styrene sulfonate) brushes varies as: $Cs^+ > K^+ > Na^+ > Li^+$.	PSS is mildly hydrophobic,[78] stemming from the fact that the significant hydrophobic nature of the styrene part of the molecule overwhelms the effect of the mildly hydrophilic part of the negatively charged sulfonate group. The degree of chaotropic nature of the cations varies as: $Cs^+ > K^+ > Na^+ > Li^+$. This explains the variation of the binding strength of the cations to the PSS brushes as $Cs^+ > K^+ > Na^+ > Li^+$.
He *et al.* (ref. 65)	Ca^{2+} (Ba^{2+}) ions bind more strongly (weakly) to the anionic COO^- group of the poly-zwitterionic poly(cysteine methacrylate) (PCysMA) brushes	Ca^{2+} ions are more kosmotropic than the Ba^{2+} ion, while COO^- is a hydrophilic group. Accordingly, Ca^{2+} ions bind more strongly to the COO^- group of the PCysMA brushes.
Xu *et al.* (ref. 66)	The strength of binding of the divalent cations to the PSS brushes varies as: $Ba^{2+} > Ca^{2+} > Mg^{2+}$.	PSS brushes are hydrophobic[48] (already discussed), while the degree of chaotropic nature of the cations varies as: $Ba^{2+} > Ca^{2+} > Mg^{2+}$. This explains the variation of the binding strength of the divalent cations to the PSS brushes as $Ba^{2+} > Ca^{2+} > Mg^{2+}$.
Bracha *et al.* (ref. 67)	The DNA brushes are found to have smaller heights in the presence of $MgCl_2$ salt than in the presence of NaCl salt, indicating that the strength of binding varied as $Mg^{2+} > Na^+$	DNA molecules contain the hydrophilic phosphate group as their charged functional group. Therefore, more kosmotropic ions will bind more strongly to the DNA brushes. Mg^{2+} is more kosmotropic than the Na^+ ion; hence Mg^{2+} binds more strongly than the Na^+ ion to the DNA brushes.
Gupta and Natarajan (ref. 72)	Li^+ ions bind more strongly than Cs^+ ions to PAA chains	PAA chains have the COO^- group that is hydrophilic; hence Li^+ ions (more kosmotropic ion) bind more strongly than the Cs^+ (less kosmotropic ion) to the PAA chains.
Kastinen *et al.* (ref. 73)	K^+ ions bind more strongly than Na^+ ions to the PSS chains (revealed by *ab initio* MD simulations)	PSS chains have hydrophobic functional groups; accordingly, the ions that are more (less) chaotropic will bind more strongly (weakly) to the PSS chains. K^+ ions are more chaotropic than Na^+ ions, and hence they will bind more strongly (than Na^+ ions) to the PSS chains.
Delgado and Schlenoff (ref. 75)	The strength of binding of the anionic counterions to the PAEDAPS [(poly(3-[2-(acrylamido)ethyldimethylammonio]-propanesulfonate))] PZI chain varies as: $SCN^- > ClO_4^- > NO_3^- > Br^- > Cl^- > SO_4^{2-}$	In PAEDAPS, the trimethyl ammonium group is the cationic part; thus, the cationic functional group is hydrophobic. Accordingly, anions that are more chaotropic will bind more strongly to the brushes. This explains why the strength of binding counterions to the PAEDAPS PZI chain varies as: $SCN^- > ClO_4^- > NO_3^- > Br^- > Cl^- > SO_4^{2-}$ (given that the degree of chaotropic nature of these ions varies as: $SCN^- > ClO_4^- > NO_3^- > Br^- > Cl^- > SO_4^{2-}$).
Kastinen *et al.* (ref. 73)	Br^- ions bind more strongly than Cl^- ions to the PDADMA [poly(diallyldimethylammonium)] chains (shown by *ab initio* MD simulations)	PDADMA chains have a hydrophobic functional group. Br^- ions are more chaotropic than Cl^- ions: this justifies their stronger binding to the PDADMA chains.

$\rho(\boldsymbol{r})$'' curve, a sudden spike in an ideal exponential-decay behavior of the curves denotes an interaction. For the case of the SCN^- ion interacting with the $\{N(CH_3)_3\}^+$ group, the spikes in the RDG($\boldsymbol{r}$) *vs.* ''$[\mathrm{sign}(\lambda_2)]\cdot\rho(\boldsymbol{r})$'' curve occur near 0 value of the ''$[\mathrm{sign}(\lambda_2)]\cdot\rho(\boldsymbol{r})$'' (green zone) denoting weak ionic interactions characterizing the SCN^-–$\{N(CH_3)_3\}^+$ binding [see Fig. 7(d and e)]. This example provides additional information on the electronic effects associated with the ion binding. Different ions (based on the monoatomic or multi-atomic nature as well as the electronic structure of each atom of the ion) will trigger different electronic effects while binding. In future studies, it will be very interesting to correlate the hydration driven binding strength with the variation in the electronic effects associated with such binding processes. For example, hydration effects determine that the SCN^- ion binds much more strongly than the SO_4^{2-} ion to the $\{N(CH_3)_3\}^+$ group of the $PMETA^+$ brushes: how the corresponding electronic effects vary (given that both the SO_4^{2-} ion and the SCN^- ion are multi-atomic ions)? Second, how will electronic effects change if, instead

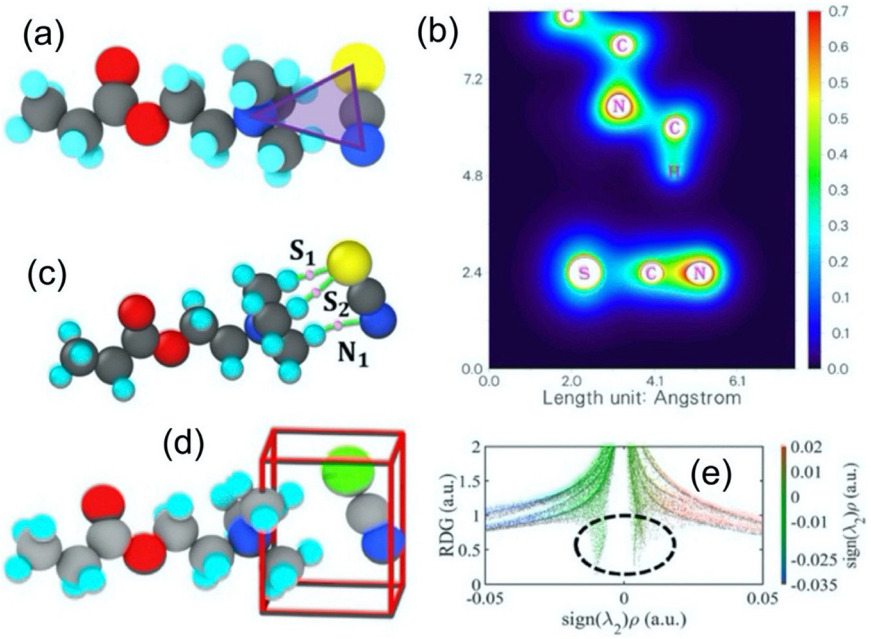

Fig. 7 (a) Representative $PMETA^+$–SCN^- ion pair system utilized for the DFT calculations. Blue, cyan, grey, red, and yellow particles, respectively, denote the nitrogen, hydrogen, carbon, oxygen, and sulfur atoms. (b) Electron density map (obtained through DFT calculations) projected on a plane that goes through the S–N–$N_{\{N(CH_3)_3\}^+}$ plane (the middle "N" is the nitrogen atom of the SCN^- ion). The color bar provides the electron density in atomic units (a.u.). QTAIM analysis of the DFT-derived electron density data confirms that there are two bond critical points (BCPs) between the S atom of the SCN^- ion and $PMETA^+$ (these BCPs are identified as S_1 and S_2) and a single BCP between the N atom of the SCN^- ion and $PMETA^+$ (this BCP is identified as N_1) (results not shown). Panel (c) shows this schematically. (d) Schematic showing SCN–$PMETA^+$ ion pair with the region enclosed by the red box being the region where the NCI analysis was performed. (e) 2D NCI plot. All subfigures have been reproduced from ref. 79 with permission from the American Chemical Society (R. Ishraaq and S. Das, Molecular dynamics simulation and density functional theory calculations of multiatomic counterion binding to cationic polyelectrolyte brushes, *J. Phys. Chem. B*, 2026, **130**, 640, copyright 2025).

of one monomer and one ion, we consider multiple monomers and multiple ions, given that in such a situation, many-body electronic interactions will be significantly augmented (please note that one will need to consider, for example, two monomers of $PMETA^+$ per molecule of the SO_4^{2-} ion for such electronic calculations in order to maintain charge neutrality)? Responses to these questions, we anticipate, will open up new paradigms of understanding of ion binding to PE brushes and PE chains.

E.2. Machine learning aided calculations

In several recent papers, we have employed supervised and unsupervised machine learning (ML) techniques on all-atom MD simulation data (on PE brush simulations) for quantifying various facets associated with the PE brushes and the brush-supported counterions and water molecules. For example, in one of our papers, we employed an unsupervised clustering algorithm to quantify the manner in which the nature of the counterions binding to the PE brushes affects the corresponding water–water hydrogen bonding inside the brush layer.[15] Our studies revealed that due to the changes in the parameters related to the PE brushes (parameters such as grafting density, charge fraction, counterion size, and counterion valence), the charge environment inside the PE brushes changed, which eventually led to the deviation of the properties of the solvent (nature of the water–water hydrogen bonds) from the bulk. In another paper, we employed linear discriminant analysis (LDA) for identifying the role of counterions in driving the non-linearly large electroosmotic (EOS) transport in nanochannels grafted with the cationic PE brushes.[60] Finally, we employed a combination of Gaussian pre-processing of data and unsupervised clustering for identifying the presence of multiple solvation states of the $\{N(CH_3)_3\}^+$ functional group of the Cl^--ion-screened cationic $PEMTA^+$ brush.[14] Specifically, there were two hydration states: one state with more structured water and another state with less structured water (see Fig. 8). The hydration state with less structured water arose from the collective interactions among multiple charged species, including the counterion, neighboring functional groups, and the $\{N(CH_3)_3\}^+$ moiety itself. In contrast, the hydration state with more structured water emerged from the relatively apolar character and the small size of the $\{N(CH_3)_3\}^+$ functional group, which enforced a wrapping configuration of the surrounding water molecules.

These examples reveal the significant capabilities of the ML methods to identify novel properties of the PE brush–counterion–water and PE chain–counterion–water systems as a function of the nature of the counterion binding to the PE brushes and chains. Therefore, an important future direction will be to use appropriate ML methods on simulation generated data (all-atom MD data or DFT-generated data) to probe the effects of varying binding interactions (between different counterions and different types of functional groups of the PE brushes) in affecting a wide range of properties of the PE brush–counterion–water or PE

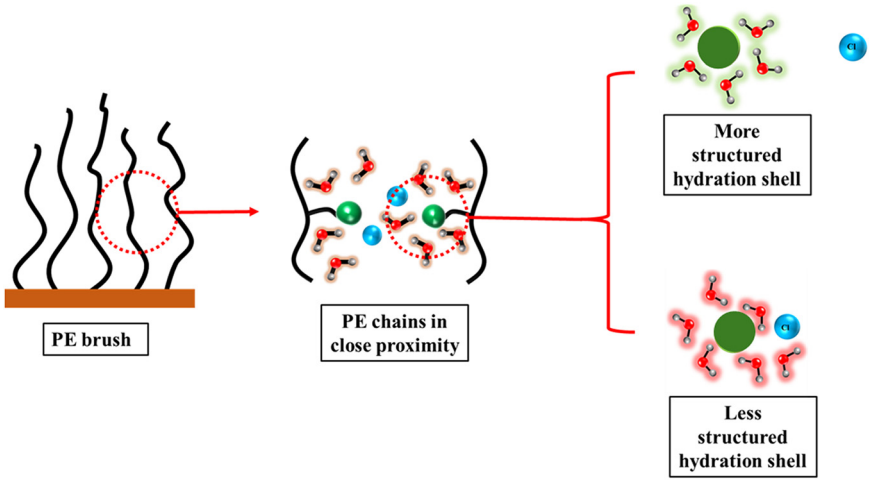

Fig. 8 Schematic showing two hydration states of the $\{N(CH_3)_3\}^+$–Cl^- ion pair, which constitutes a more structured and a less structured hydration shell. This figure has been adapted from ref. 14 with permission from the American Chemical Society (R. Ishraaq, T. S. Akash, and S. Das, Combined machine learning and molecular dynamics reveal two states of hydration of a single functional group of cationic polymeric brushes, *Macromolecules*, 2024, **57**, 5300, copyright 2024).

chain–counterion–water systems (properties such as water–water and water–counterion hydrogen bonding inside the brush layer, hydration/solvation states of the PE functional group as well as the counterions, *etc.*)

E.3. Applications

The ability to predict the strength of binding of counterions to the PE brushes (or the PE chains) by tallying the nature of the counterions (how much kosmotropic/chaotropic they are) to the hydrophobicity/hydrophilicity of the functional groups of the PE brushes (or PE chains) can be extremely useful for making predictions about a number of events involving such counterion-screened PE brush (or PE chain) systems. We list below a few that have generated significant interests in the community.

E.3.1. Change in the brush configuration (if any) by the addition of an external salt. Using our hypothesis, we can predict what will happen to the configuration of the brushes (screened with certain types of counterions) when one adds to the system a salt containing an ion (anion or cation) that can serve as a (different) counterion to the PE brushes. Let us explain it using an example.

Consider a cationic brush with a hydrophobic charged functional group [*e.g.*, $PMETA^+$ brushes having the hydrophobic $\{N(CH_3)_3\}^+$ group] screened with an anion B^- (B^- can be either a monoatomic ion like Cl^- or a multi-atomic ion like SCN^-). Under these circumstances, let the brush height be h_B. At this point, consider adding a salt that has an anion D^- (D^- can be either a monoatomic ion or a multi-atomic ion), and let the resulting brush height be h_D. The question is, based on our hypothesis, can we predict if $h_D > h_B$, or $h_D < h_B$, or $h_D \sim h_B$ if we know the nature (chaotropic or kosmotropic) of the anions B^- and D^-. Consider that the B^- ion is more chaotropic than the D^- ions. Therefore, the D^- ion will bind much more weakly (than the B^- ion) to the brush having the hydrophobic charged functional group. Hence, it would be unlikely that the D^- ion will replace the B^- ion as the screening counterion of the brushes (having a hydrophobic charged functional group). Under these circumstances, there is less chance that there will be much change in the brush configuration, and hence for this case, $h_D \sim h_B$. Let us now consider the case, where the D^- ions are more chaotropic than the B^- ions: accordingly, D^- ions will bind more strongly to the PE brushes, and therefore will replace at least some of the original screening counterions (B^- ions). Under these circumstances it is likely that some of the salt can enter the brush layer, given that the replacement of the B^- ions with the D^- ions (as the counterions screening the PE brush charge) is more favorable. When all or some of the brush charges are now screened by the D^- ions (which are more chaotropic), the binding of the screening ions to the brush charges is much stronger. As a result, the extent of the screening of the PE brush charges is much stronger as compared to the case where the B^- ions were screening the brush charges by being loosely bound to the brushes. For this former case (case when B^- ions were the screening counterions), this looser binding of the counterions and weaker extent of screening would have meant that the inter-monomer repulsion is stronger causing the brushes to swell. Therefore, when the D^- ions become the screening counterions, the stronger binding of the counterions and the associated greater degree of screening will imply that the inter-monomer repulsion is significantly reduced, thereby compressing the brush layer. Thus, for this case, $h_D < h_B$.

We can discuss similar situations for the case when the PE brushes have hydrophilic functional groups. For that case (considering cationic brushes; for example, PAH brushes), $h_D \sim h_B$ if the B^- ion is more kosmotropic (less chaotropic) than the D^- ion (with the added salt showing little tendency to enter the brush layer), while $h_D < h_B$ if the B^- ion is less kosmotropic (more chaotropic) than the D^- ion (with the added salt showing a strong tendency to enter the brush layer).

Table 2 Summary of the expected changes in the brush heights with added salt: use of our hypothesis

Type of PE brush	Nature of original screening counterion	Nature of the counterion coming from the added salt	Expected change in brush height
Cationic (anionic) brushes with hydrophobic functional groups	More chaotropic	Less chaotropic	Little change in brush height with the added salt not entering the brush layer
Cationic (anionic) brushes with hydrophobic functional groups	Less chaotropic	More chaotropic	Brush height should decrease with added salt entering the brush layer and the screening counterions getting replaced by the counterions introduced by the salt
Cationic (anionic) brushes with hydrophilic functional groups	More kosmotropic	Less kosmotropic	Little change in brush height with added salt not entering the brush layer
Cationic (anionic) bushes with hydrophilic functional groups	Less kosmotropic	More kosmotropic	Brush height should decrease with added salt entering the brush layer and the screening counterions getting replaced by the counterions introduced by the salt

The same logic holds true for the case of anionic brushes with either hydrophilic functional groups (*e.g.*, PAA brushes) or hydrophobic functional groups (*e.g.*, PSS brushes). Let's say that the original screening counterions is E^+ (the corresponding height is h_E) and the added salt has the cation F^+ (and the brush height after the addition of this salt is h_F). Then by the logic discussed above, for the case of the anionic brushes with hydrophobic functional groups, $h_E \sim h_F$ if the E^+ ion is more chaotropic than the F^+ ion (with the added salt showing little tendency to enter the brush layer), while $h_F < h_E$ if the E^+ ion is less chaotropic than the F^+ ion (with the added salt showing a strong tendency to enter the brush layer). On the other hand, for the case of the anionic brushes with hydrophilic functional groups, $h_E \sim h_F$ if the E^+ ion is more kosmotropic (less chaotropic) than the F^+ ion (with the added salt showing little tendency to enter the brush layer), while $h_F < h_E$ if the E^+ ion is less kosmotropic (more chaotropic) than the F^+ ion (with the added salt showing a strong tendency to enter the brush layer).

The discussions made in this section are summarized in Table 2.

E.4. Protein binding to similarly charged PE chains and brushes

The binding of proteins to the PE chains and brushes has been studied extensively. The most interesting type of binding happens when the proteins bind to the like-charged PE brushes (*e.g.*, a net negatively charged protein binds to a net negatively charged PE brush).[82–87] For example, net negatively charged β-lactoglobulin (BLG) protein binds to the anionic spherical PSS (poly-styrene sulfonate brushes) brushes (*i.e.*, PSS brushes grafted to a spherical particle).[82] Such binding becomes possible because the BLG protein, although net negative, has patches of densely packed positive charges on the protein surface and the BLG interacts with this positive patch with the negatively charged spherical PSS brushes. Under these conditions, this positively charged patch behaves as a multivalent counterion (due to the fact that like multivalent counterion, this positively charged patch has a much larger charge density) and binds to the PSS by displacing the (typically) monovalent counterions that were originally screening the charges of the PSS brush layer. This is an overall thermodynamically favorable process due to two factors: (1) the strength of binding of the charged patch (due to its multi-valent nature) to the PSS functional group is significantly greater than the strength of binding between the monovalent counterion and PSS and (2) a significant number of counterions become free (*i.e.*, get released) [for example, if the patch is behaving as a tri-valent entity, prior to adhering to the brushes, the patch is screened by 3 monovalent counterions; thus when it binds to the PSS brushes, a total of $2 \times 3 = 6$ counterions are released]. The process is described in Fig. 9.

Unfortunately, in this framework involving PSS or other types of brushes, the hydration effects of the PSS (or other brushes), protein charged patch, and the counterions involved have not been considered at all. The significance of this consideration will come to the fore if we provide an example where such protein binding to the PE brushes (or PE chains) will fail due to disregard of this hydration effect. Consider that the charged functional group of the brush is a hydrophobic one (*e.g.*, the case of the PSS brushes) and a chaotropic ion (*e.g.*, Cs^+ ion) is bound to the PSS (as the original screening monovalent counterion). Let us now consider that the positively charged patch of the protein is hydrophilic in nature and the counterions bound to the patch are kosmotropic in nature (*e.g.*, F^- ions). Therefore, if this positively charged patch, in order to bind to the brushes, comes to replace the Cs^+ ion, it would mean that a hydrophilic charged patch (serving as a multivalent counterion) will need to bind to a hydrophobic functional group (of the PSS brushes) by replacing a chaotropic ion that was originally bound to the hydrophobic functional group. Such a thing might not be energetically permissible.

Thus, to engineer any situation that aims to ensure the binding of a charged protein (or other macroions, such as charged surfactants) to the PE chains and brushes, one should address these hydration issues associated with the PE brushes (PE chains), the binding entities (*e.g.*, charged proteins), and the involved counterions (counterions screening the charges of the PE brushes or PE chains as well as the counterions screening the charges of the proteins that bind to the brushes/chains).

E.5. Limitations of the proposed hypothesis

There are cases where the proposed hypothesis does not work perfectly. For example, Kou *et al.* considered the variation of the $PMETA^+$ brush height for counterions that become progressively more chaotropic from kosmotropic (namely, SO_4^{2-},

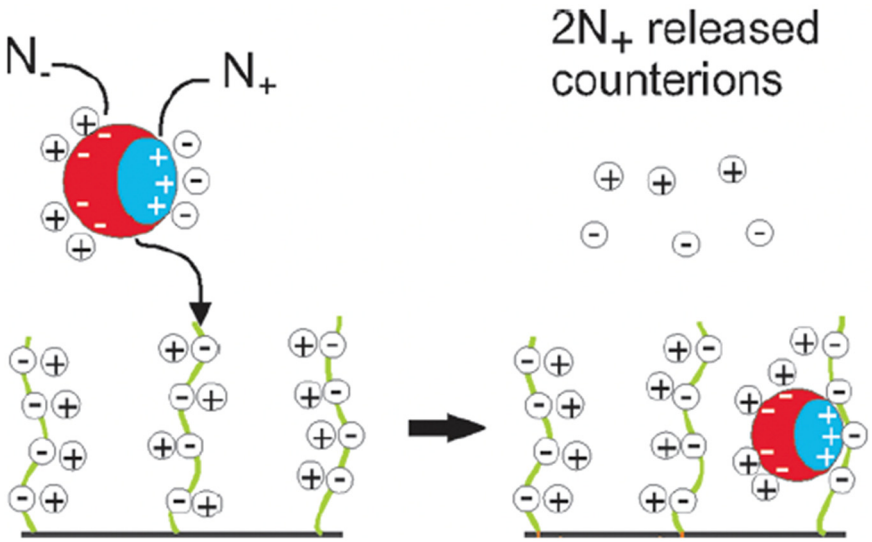

Fig. 9 Schematic illustration showing the binding of proteins to the like-charged PE brushes. The protein is net negative; however, it contains a patch of positive charges. During the binding, the positively charged patch on the protein surface acts as a multivalent cation that binds to the PE brushes (thereby screening the brush charges). If the patch has N_+ number of positive charges (here $N_+ = 3$), this binding releases N_+ negative counterions that were originally screening this positive patch and N_+ positive counterions from the brush layer. Thus, there is a total release of $2N_+$ (=6) counterions. This figure has been adapted from ref. 82 with permission from the American Chemical Society (K. Henzler, B. Haupt, K. Lauterbach, A. Wittemann, O. Borisov, and M. Ballauff, Adsorption of β-lactoglobulin on spherical polyelectrolyte brushes: direct proof of counterion release by isothermal titration calorimetry, *J. Am. Chem. Soc.*, 2010, **132**, 3159, copyright 2010).

HPO_4^{2-}, CH_3COO^-, Cl^-, Br^-, NO_3^-, I^-, and SCN^-).[44] The brush height, however, does not monotonically decrease from SO_4^{2-} to SCN^-, while our hypothesis would have suggested that the brush height should progressively decrease as one goes from more kosmotropic to more chaotropic ions. The experimental findings of Kou *et al.*'s paper show that the brush height for different salt concentrations (salt that furnishes this counterion) first increases (very slowly) as one goes from SO_4^{2-} to HPO_4^{2-} to CH_3COO^-, but after that the height progressively decreases as one goes from CH_3COO^- to Cl^- to Br^- to NO_3^- to I^- to SCN^-. This progressive decrease is commensurate with our proposed hypothesis: more the chaotropic ion, stronger will be its binding to the $PMETA^+$ brushes (due to the presence of the hydrophobic group of the $PMETA^+$ brushes). Of course, this deviation, which is primarily between the cases of the multivalent counterion (SO_4^{2-} and HPO_4^{2-}) and monovalent counterion (CH_3COO^-), might be due to the much greater charge density of the divalent counterions. Such enhanced charge density (of the divalent counterions) will imply that the electrostatic interactions might (partially) overwhelm the hydration effects, and thus, the binding strength does not increase monotonically as one moves from SO_4^{2-} to HPO_4^{2-} to CH_3COO^- counterions.

There are other examples where the electrostatic interactions become the dominant factor, instead of the hydration effects, and for such cases our hypothesis might fail. One example is the study of Ehtiati *et al.*,[45] where it was found that for a smaller brush grafting density (0.08 nm^{-2}) and lower salt concentrations (less than 0.1 M), the poly[2-(1-butylimidazolium-3-yl)ethyl methacrylate] brush height varied as: $(h_b)_{SCN^-} < (h_b)_{Br^-} < (h_b)_{NO_3^-} < (h_b)_{Cl^-}$, despite the fact that the functional group of the brush is hydrophobic (see Table 1), while the NO_3^- ion is more chaotropic than the Br^- ion [and hence, according to our hypothesis, one would have expected $(h_b)_{Br^-} > (h_b)_{NO_3^-}$]. This happens due to a combination of weak grafting density and low salt concentration. Such a weak grafting density implies the presence of a significant amount of space between the grafted brushes, while a low salt concentration implies that a relatively less amount of salt enters the brush layer. Under these conditions, the NO_3^- ion can move around much more freely inside the brush layer and can interact with the brush functional group with any of its oxygen atoms. This makes the electrostatic binding somewhat weak stemming from the fact that the charge of the NO_3^- ion is distributed on the three oxygens. In contrast, the charge is localized on the Br^- ion (as it is a single-atom ion) and therefore, the electrostatics-driven binding of the Br^- ion to the brush-functional group is stronger. This justifies why $(h_b)_{Br^-} < (h_b)_{NO_3^-}$. However, the moment the grafting density becomes high or the salt concentration becomes high, there is not enough space (for a given ion) within the brush layer to enforce such freer motion of the ions within the brush layer, and accordingly, the dominant hydration effects ensure $(h_b)_{Br^-} > (h_b)_{NO_3^-}$ (*i.e.*, something suggested by our hypothesis).

F. Conclusions

In this perspective article, we provide and test a hypothesis aimed at identifying the ion-specific effects that determine which ion will undergo a more favorable binding to the PE brushes and PE chains having a specific type of functional group. More specifically, we hypothesize that ions that are more chaotropic (kosmotropic) in the Hoffmeister series will bind

more favorably to the PE brushes and PE chains having hydrophobic (hydrophilic) functional groups. Our hypothesis is based on the principle that the chaotropic (kosmotropic) ions disrupt (preserve) the water structure more efficiently, and therefore, by the law of matching water affinity, bind more favorably to hydrophobic (hydrophilic) functional groups, *i.e.*, functional groups that have a similar disruptive (preserving) effect on the water structure. This paper, therefore, points to the role of hydration in determining which ion will bind more favorably to PE brushes and PE chains. We cite results from several experimental and *ab initio* simulation papers and test our hypothesis against these results: these results are found to strongly support our hypothesis. Finally, we point out (1) how the understanding of the science of ion binding to PE chains and brushes can be further enriched by carrying out DFT and ML calculations and (2) identify several applications (*e.g.*, exchange of ions serving as screening counterions of the PE chains and brushes, protein–PE brush and protein–PE chain interactions) that will benefit from our proposed hypothesis.

Conflicts of interest

There are no conflicts to declare.

Data availability

No primary research results, software or code have been included and no new data were generated or analysed as part of this perspective article.

Acknowledgements

This work has been supported by the U.S. Department of Energy Office of Science grant DE-SC0017741.

References

1 S. Das, M. Banik, G. Chen, S. Sinha and R. Mukherjee, *Soft Matter*, 2015, **11**, 8550.
2 L. A. Smook, A. Dahlin, K. Schroën and S. de Beer, *Adv. Mater.*, 2025, **37**, e09580.
3 M. Tirrell, *ACS Cent. Sci.*, 2018, **4**, 532.
4 B. Sim, J. J. Chang, Q. Lin, J. H. M. Wong, V. Ow, Y. Leow, Y. J. Wong, Y. J. Boo, R. Goh and X. J. Loh, *Biomacromolecules*, 2024, **25**, 7563.
5 N. Wanasingha, P. Dorishetty, N. K. Dutta and N. R. Choudhury, *Gels*, 2021, **7**, 148.
6 H. S. Sachar, T. H. Pial, P. R. Desai, S. A. Etha, Y. Wang, P. W. Chung and S. Das, *Matter*, 2020, **2**, 1509.
7 H. S. Sachar, T. H. Pial, B. S. Chava and S. Das, *Soft Matter*, 2020, **16**, 7808.
8 H. S. Sachar, B. S. Chava, T. H. Pial and S. Das, *Macromolecules*, 2021, **54**, 6342.
9 T. H. Pial, H. S. Sachar and S. Das, *Macromolecules*, 2021, **54**, 4154.
10 H. S. Sachar, B. S. Chava, T. H. Pial and S. Das, *Macromolecules*, 2021, **54**, 2011.
11 R. Ishraaq, T. S. Akash, A. Bera and S. Das, *J. Phys. Chem. B*, 2024, **128**, 381.
12 T. H. Pial and S. Das, *Soft Matter*, 2022, **18**, 8945.
13 R. Ishraaq and S. Das, *Macromolecules*, 2024, **57**, 3037.
14 R. Ishraaq, T. S. Akash and S. Das, *Macromolecules*, 2024, **57**, 5300.
15 A. Bera, T. S. Akash, R. Ishraaq and S. Das, *Macromolecules*, 2024, **57**, 1581.
16 E. B. Zhulina and M. Rubinstein, *Macromolecules*, 2014, **47**, 5825.
17 E. B. Zhulina, O. V. Borisov and T. M. Birshtein, *Macromolecules*, 1999, **32**, 8189.
18 N. A. Kumar and C. Seidel, *Macromolecules*, 2005, **38**, 9341.
19 C. Seidel, *Macromolecules*, 2003, **36**, 2536.
20 M. Ballauff, *Prog. Polym. Sci.*, 2007, **32**, 1135.
21 B.-Y. Ha and D. Thirumalai, *Macromolecules*, 1995, **28**, 577.
22 S. W. Cranford and M. J. Buehler, *Macromolecules*, 2012, **45**, 8067.
23 P. R. Desai, S. Sinha and S. Das, *Phys. Rev. E*, 2018, **97**, 032503.
24 G. Chen and S. Das, *J. Phys. Chem. B*, 2015, **119**, 12714.
25 J. Chen, M. Duan, R. Zhang and G. Chen, *Macromolecules*, 2026, DOI: 10.1021/acs.macromol.6c00048.
26 S. Misra, S. Varanasi and P. P. Varanasi, *Macromolecules*, 1989, **22**, 4173.
27 P. Pincus, *Macromolecules*, 1991, **24**, 2912.
28 R. S. Ross and P. Pincus, *Macromolecules*, 1992, **25**, 2177.
29 O. V. Borisov, T. M. Birshtein and E. B. Zhulina, *J. Phys. II*, 1991, **1**, 521.
30 E. B. Zhulina and M. Rubinstein, *Soft Matter*, 2012, **8**, 9376.
31 S. A. Etha, V. S. Sivasankar, H. S. Sachar and S. Das, *Phys. Chem. Chem. Phys.*, 2020, **22**, 13536.
32 H. S. Sachar, V. S. Sivasankar and S. Das, *Soft Matter*, 2019, **15**, 559.
33 J. D. Willott, T. J. Murdoch, B. A. Humphreys, S. Edmondson, E. J. Wanless and G. B. Webber, *Langmuir*, 2015, **31**, 3707.
34 K. Ehtiati, S. Z. Moghaddam, A. E. Daugaard and E. Thormann, *Macromolecules*, 2021, **54**, 3388.
35 X. He, K. Zhang, Y. Liu, F. Wu, P. Yu and L. Mao, *Angew. Chem.*, 2018, **130**, 4680.
36 M. Balastre, F. Li, P. Schorr, J. Yang, J. W. Mays and M. V. Tirrell, *Macromolecules*, 2002, **35**, 9480.
37 F. S. Samghabadi, S. R. Bajgiran, M. V. Orellana, J. C. Conrad and A. B. Maricel, *ACS Macro Lett.*, 2024, **13**, 1570.
38 V. M. dos Santos, E. R. Almeida, L. M. P. Souza, A. S. Pimentel, M. Ramstedt and T. A. Soares, *Macromolecules*, 2025, **58**, 5431.
39 D. J. Sandberg, J.-M. Y. Carrillo and A. V. Dobrynin, *Langmuir*, 2007, **23**, 12716.
40 T. Kinjo, H. Yoshida and H. Washizu, *Colloid Polym. Sci.*, 2018, **296**, 441.
41 L. A. Smook and S. de Beer, *Macromolecules*, 2025, **58**, 1185.
42 L. A. Smook and S. de Beer, *J. Polym. Sci.*, 2025, **63**, 3446.
43 C. Ji, C. Zhou, B. Zhao, J. Yang and J. Zhao, *Langmuir*, 2021, **37**, 5554.

44 R. Kou, J. Zhang, T. Wang and G. Liu, *Langmuir*, 2015, **31**, 10461.
45 K. Ehtiati, S. Z. Moghaddam, H.-A. Klok, A. E. Daugaard and E. Thormann, *Macromolecules*, 2022, **55**, 5123.
46 J. Yu, J. Mao, G. Yuan, S. Satija, Z. Jiang, W. Chen and M. Tirrell, *Macromolecules*, 2016, **49**, 5609.
47 X. Xu, D. Mastropietro, M. Ruths, M. Tirrell and J. Yu, *Langmuir*, 2019, **35**, 15564.
48 Y. Mei, K. Lauterbach, M. Hoffmann, O. V. Borisov, M. Ballauff and A. Jusufi, *Phys. Rev. Lett.*, 2006, **97**, 158301.
49 R. Farina, N. Laugel, J. Yu and M. Tirrell, *J. Phys. Chem. C*, 2015, **119**, 14805.
50 J. Yu, N. E. Jackson, X. Xu, B. K. Brettmann, M. Ruths, J. J. de Pablo and M. Tirrell, *Sci. Adv.*, 2017, **3**, eaao1497.
51 J. Yu, N. E. Jackson, X. Xu, Y. Morgenstern, Y. Kaufman, M. Ruths, J. J. de Pablo and M. Tirrell, *Science*, 2018, **360**, 1434.
52 R. Ishraaq and S. Das, *Phys. Chem. Chem. Phys.*, 2025, **27**, 22901.
53 T. H. Pial and S. Das, *J. Phys. Chem. B*, 2022, **126**, 10543.
54 B. Kang, H. Tang, Z. Zhao and S. Song, *ACS Omega*, 2020, **5**, 6229.
55 Y. Marcus, *Chem. Rev.*, 2009, **109**, 1346.
56 T. H. Pial, M. Prajapati, B. S. Chava, H. S. Sachar and S. Das, *Macromolecules*, 2022, **55**, 2413.
57 H. S. Sachar, T. H. Pial, V. S. Sivasankar and S. Das, *ACS Nano*, 2021, **15**, 17337.
58 T. H. Pial, H. S. Sachar, P. R. Desai and S. Das, *ACS Nano*, 2021, **15**, 6507.
59 R. Ishraaq and S. Das, *Chem. Commun.*, 2024, **60**, 6093.
60 R. Ishraaq and S. Das, *J. Phys. Chem. B*, 2025, **129**, 5854.
61 R. Ishraaq and S. Das, *ACS Appl. Polym. Mater.*, 2025, **7**, 2797.
62 H. Mori, M. Wakagawa, S. Kuroki and M. Satoh, *Colloid Polym. Sci.*, 2015, **293**, 1023.
63 K. Satoh, S. Kuroki and M. Satoh, *Colloid Polym. Sci.*, 2015, **293**, 1453.
64 M. Hayashi, M. Wakagawa, T. Minato, Y. Nishiyama, S. Kuroki and M. Satoh, *J. Polym. Sci., Part B*, 2009, **47**, 2122.
65 Q. He, Y. Qiao, C. M. Jimenez, R. Hackler, A. B. F. Martinson, W. Chen and M. V. Tirrell, *Macromolecules*, 2023, **56**, 1945.
66 X. Xu, D. Mastropietro, M. Ruths, M. Tirrell and J. Yu, *Langmuir*, 2019, **35**, 15564.
67 D. Bracha, E. Karzbrun, G. Shemer, P. A. Pincus and R. H. Bar-Ziva, *Proc. Natl. Acad. Sci. U. S. A.*, 2013, **10**, 4534.
68 A. Chhabra, S. Mandal, Y. Zhang and O. Gang, *Small*, 2026, e12678, DOI: 10.1002/smll.202512678.
69 N. Srinivasan, M. Bhagawati, B. Ananthanarayanan and S. Kumar, *Nat. Commun.*, 2014, **5**, 5145.
70 T. J. Yokokura, C. Duan, E. A. Ding, S. Kumar and R. Wang, *Biomacromolecules*, 2024, **25**, 328.
71 C. Pradal, G. E. Yakubov, M. A. K. Williams, M. A. McGuckin and J. R. Stokes, *Biotribology*, 2019, **18**, 100092.
72 A. K. Gupta and U. Natarajan, *Mol. Simul.*, 2017, **43**, 625.
73 T. Kastinen, P. Batys, D. Tolmachev, K. Laasonen and M. Sammalkorpi, *Chem. Phys. Chem.*, 2024, **25**, e202400244.
74 Y. Nishiyama and M. Satoh, *Macromol. Rapid Commun.*, 2000, **21**, 174.
75 J. D. Delgado and J. B. Schlenoff, *Macromolecules*, 2017, **50**, 4454.
76 P. Loh, G. R. Den, D. Vollmer, K. Fischer, M. Schmidt, A. Kundagrami and M. Muthukumar, *Macromolecules*, 2008, **41**, 9352.
77 S. Tu, S. S. Lobanov, J. Bai, H. Zhong, J. Gregerson, A. D. Rogers, L. Ehm, B. John and J. B. Parise, *J. Phys. Chem. B*, 2019, **123**, 9654.
78 H. Ahrens, K. Büscher, D. Eck, S. Förster, C. Luap, G. Papastavrou, J. Schmitt, R. Steitz and C. A. Helm, *Macromol. Symp.*, 2004, **211**, 93.
79 R. Ishraaq and S. Das, *J. Phys. Chem. B*, 2026, **130**, 640.
80 P. S. V. Kumar, V. Raghavendra and V. Subramanian, *J. Chem. Sci.*, 2016, **128**, 1527.
81 S. Vargas, W. Gee and A. Alexandrova, *Digital Discovery*, 2024, **3**, 987–998.
82 K. Henzler, B. Haupt, K. Lauterbach, A. Wittemann, O. Borisov and M. Ballauff, *J. Am. Chem. Soc.*, 2010, **132**, 3159.
83 C. Yigit, M. Kanduc, M. Ballauff and J. Dzubiella, *Langmuir*, 2017, **33**, 417.
84 C. Yigit, J. Heyda, M. Ballauff and J. Dzubiella, *J. Chem. Phys.*, 2015, **143**, 064905.
85 A. Wittemann and M. Ballauff, *Phys. Chem. Chem. Phys.*, 2006, **8**, 5269.
86 A. Wittemann, B. Haupt and M. Ballauff, *Phys. Chem. Chem. Phys.*, 2003, **5**, 1671.
87 K. Radhakrishnan and C. Holm, *Macromolecules*, 2025, **58**, 13222.